

Nanoscale

Accepted Manuscript



This is an *Accepted Manuscript*, which has been through the Royal Society of Chemistry peer review process and has been accepted for publication.

Accepted Manuscripts are published online shortly after acceptance, before technical editing, formatting and proof reading. Using this free service, authors can make their results available to the community, in citable form, before we publish the edited article. We will replace this *Accepted Manuscript* with the edited and formatted *Advance Article* as soon as it is available.

You can find more information about *Accepted Manuscripts* in the [Information for Authors](#).

Please note that technical editing may introduce minor changes to the text and/or graphics, which may alter content. The journal's standard [Terms & Conditions](#) and the [Ethical guidelines](#) still apply. In no event shall the Royal Society of Chemistry be held responsible for any errors or omissions in this *Accepted Manuscript* or any consequences arising from the use of any information it contains.

ARTICLE

White-light Induced Grafting of 3-MPA on Si(111)-H Surface for Catalyzing Au Nanoparticles In-Situ Growth

Cite this: DOI: 10.1039/x0xx00000x

Received 00th January 2012,
Accepted 00th January 2012

DOI: 10.1039/x0xx00000x

www.rsc.org/

Li-Kun Yang, Ya-Qiong Su, Xiao-Ying Wu, Da-Xiao Zhang, Yan-Li Chen, Fang-Zu Yang*, De-Yin Wu*, and Zhong-Qun Tian

A novel, mild and effective method was designed for grafting of high-quality organic monolayers on silicon surface to catalyze nanoparticles growth. By using white-light source, 3-mercaptopropionic acid (3-MPA) molecules were attached to hydrogen-terminated Si(111) surfaces at room temperature. The attached monolayers were characterized using X-ray photoelectron spectroscopy to provide detailed information. Au nanoparticles (AuNPs) with dimensions below 20 nm were catalyzed in-situ growth on silicon surface with highly uniform and compact structure morphology. The AuNPs can grow selectively in a certain region on a patterned Si-Si₃N₄ chip. And *p*-nitrothiophenol (*p*-NTP) was used as the probe to evaluate the SERS enhancement of this highly uniform and compact AuNPs-Si substrate. In order to better understand the white light initiation of the addition reaction of 3-MPA on the Si(111)-H surface, the mechanism was elucidated by density functional theoretical (DFT) calculations which indicated that the formation of the Si–O bond occurred at the PEC of the first singlet excited state (S₁) with a very low activation barrier about 30% of the ground state (S₀) value.

Introduction

Photoinjection of hot plasmonic carriers from metal nanostructures into semiconductors is a very interesting and active topic, because it has direct relevance to semiconductor electronics,¹⁻⁵ solar cells,⁶ solid-state devices,⁷ and optical sensors. In many of these applications, hot electrons are created on a metal surface and then collected into a semiconductor to produce useful work. However, it is difficult to efficiently extract hot electrons. The motion of a hot plasmonic carrier through a metal/semiconductor interface is hampered by the presence of a potential energy barrier known as the Schottky barrier. The height of the Schottky barrier depends on the electronic properties of the interfacing materials and hot carriers must possess enough energy to overcome it to move from the metal into the conduction band of the semiconductor.⁸⁻¹²

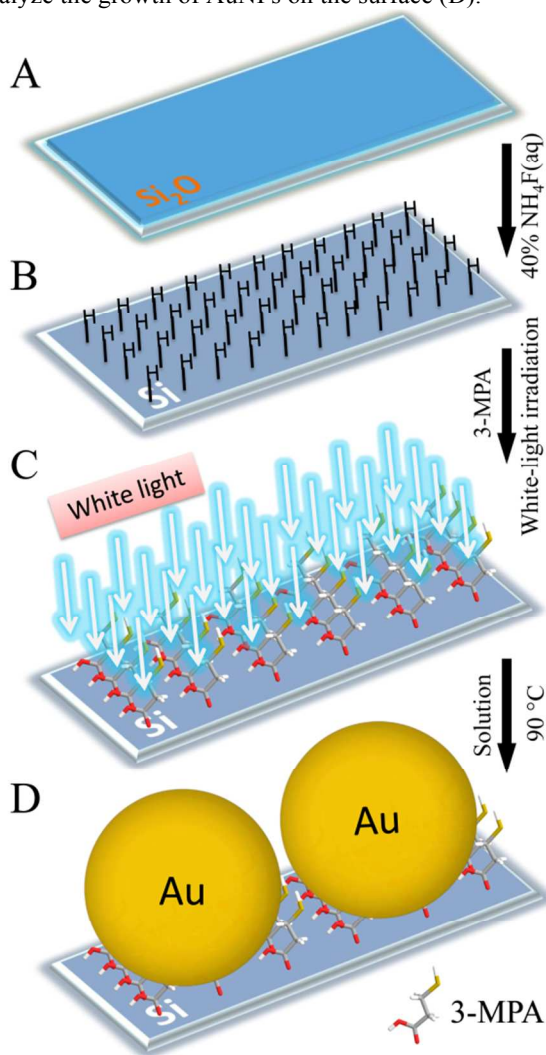
Gold nanoparticles (AuNPs) exhibit large absorption cross sections to enhance light trapping.¹³⁻¹⁵ A recent research found that only small nanoparticles with dimensions below 20 nm can efficiently generate hot electrons with large energies.^{16, 17} Nanoparticles of small size have the ability to destroy the momentum conservation in the process of interaction between phonons and confined electrons. Besides, AuNPs show unique optical properties like the localized surface plasmon resonance (LSPR) in visible light. Thus the LSPR effect results in

significant improvement in their unique optical/electronic properties of silicon-based nanostructures, so that the AuNP-Si system exhibits the potential applications in integrating LSPR with semiconductor electronics, solar cells, and optical sensors. However, it is really a challenge to fabricate small nanoparticles onto semiconductor with highly uniform and compact structure morphology. Till now, there are three strategies for fabricating the AuNPs (>50 nm) on silicon substrate.¹⁸ One strategy is to firstly modify the Si substrate with a thiol-terminated monolayer, and then AuNPs can be grafted covalently onto this substrate via Au–S bonds through thermodynamics reactions.^{3, 19} The second strategy is to graft molecule-modified AuNPs onto hydrogen-terminated silicon (Si–H) surfaces by forming Si–C bonds under light irradiation.²⁰ The third strategy is to directly assemble AuNPs by interfacial interaction, fabricating uniform NPs films on silicon surfaces.²¹⁻²³ These proposed strategies can be used to construct different metal/semiconductor interfaces, but hot electrons with low energies generated by large AuNPs cannot destroy the momentum conservation in the process of interaction between phonons and confined electrons.

In this reported work, we describe a novel, mild and effective method to graft high-quality organic monolayers on a silicon surface catalyzing small size of nanoparticles in-situ growth. The designed synthetic strategy can be readily employed using

three consecutive steps as shown in Scheme 1. In brief, the cleaned Si(111) sample is first immersed into 40% ammonium fluoride (NH_4F) solution to remove the oxide layers and generate Si-H bonds onto the surfaces of the strips (A \rightarrow B).^{18, 19, 24-27} Next, the Si(111)-H surface is modified using 3-mercaptopropionic acid (3-MPA) molecules (B \rightarrow C) at room temperature under white-light irradiation for 1 h. The resultant 3-MPA-modified Si(111) sample, acts as ligands,^{28, 29} for the Au^+ ions and reacting further with these to form crystal nuclei. The AuNPs are grown in situ on the Si surface in few minutes (C \rightarrow D).^{20, 30} It should be noted that the mild white light source was used to induce photochemical grafting of the 3-MPA bifunctional molecule, so the white-light driven reaction mechanism was analyzed, in this work, on the basis of DFT calculations.

Scheme 1. The strategy for grafting of a high-quality organic monolayer on a silicon surface to catalyze nanoparticle growth. From a cleaned Si(111) wafer (A), an atomically smooth Si(111)-H surface is made (B), which can be modified by 3-MPA molecules under a white-light irradiation (C), and then to catalyze the growth of AuNPs on the surface (D).



Experimental section

Equipment: White-light used for the grafting reaction was generated using a 125 W fluorescent work light. X-ray photoelectron spectroscopy (XPS) data were obtained on a PHI Quantum 2000 x-ray photoelectron spectrometer ($P < 5 \times 10^{-10}$ Torr) using a monochromatic Al K_{α} radiation (10 kV) with a 200 μm spot. Scanning electron microscopy (SEM) images were obtained with a Hitachi S-4800 SEM ($P < 10^{-8}$ Torr) with an accelerating voltage of 15 kV. Metallographic microscopy image was obtained with a Sunny MX6R upright metallurgical microscope. Silicon nitride (Si_3N_4) was deposited by Thermco Nitride Low Pressure Chemical Vapor Deposition (LPCVD) system. A Surface Coating Systems G3 spin coater was used to spin-coate AZ5214E photoresist. A Karl Suss MA6 mask aligner was used to realize UV-lithography. The baking process was conducted with IKA electric heating panel. Alcatel AMS200 etcher with an optimized Deep Reactive Ion Etching (DRIE) system was used to conduct Inductively Coupled Plasma (ICP) Etching.

Materials: Single-polished Si(111): n-type, Sb-doped, $450 \pm 15 \mu\text{m}$ thick, resistivity 0.01-0.02 $\Omega \cdot \text{cm}$ (Addison Engineering, CA). Ethanol (absolute), mesitylene (>99.5%), dichloromethane (>99.5%), potassium dicyanoaurate (99%), potassium citrate tribasic monohydrate (>99.5%), citric acid monohydrate (>99.5%), sulfuric acid (98%, AR), hydrogen peroxide (30%, AR) were purchased from the Sinopharm Chemical Reagent Co., Ltd. (Shanghai, China). 3-mercaptopropionic acid (99%), *p*-nitrothiophenol (>99.5%), and ammonium fluoride (40%, AR) were purchased from Aldrich.

Preparation and Functionalization of Si(111)-H: Si(111) wafers were cut into $1 \times 1 \text{ cm}^2$ pieces and cleaned in piranha solution ($\text{H}_2\text{SO}_4:\text{H}_2\text{O}_2=3:1$) at 90 °C for 1 h, subsequently etched by using 40% NH_4F for 10 min, and dried with a stream of argon gas. The 3-MPA solution was flushed with Ar for 30 min before and for 30 min after putting the fresh Si(111)-H wafer into the solution, before the light was turned on. The grafting reaction was performed by irradiation of a wafer-containing 20% (vol) solution of 3-MPA in mesitylene with white-light for 1 h under an Ar atmosphere. Afterwards, the surface was excessively rinsed with CH_2Cl_2 and EtOH, and dried with a stream of argon gas.

In-situ growth of AuNPs on Functionalized Si(111)-H surface: 3-MPA-modified Si(111) wafers were put into a solution of $\text{KAu}(\text{CN})_2$ (2.5 mM/5 mM), potassium citrate (77 mM), citric acid (32 mM) and heated at 90 °C for 10 min/20 min. Then the wafers were excessively rinsed with ultrapure water and dried with a stream of argon gas.

Process flow for fabricating a patterned chip: 4 inch silicon wafer was soaked in Piranha solution ($\text{H}_2\text{SO}_4:\text{H}_2\text{O}_2=3:1$), and rinsed by deionized water, dried by nitrogen blowing. 100 nm silicon nitride was deposited by Low Pressure Chemical Vapor Deposition (LPCVD), then AZ5214E photoresist was spin-

coated on the wafer at 2000 rpm for 30s. After baking at 96 °C for 4 mins, XMU patterns were generated by UV-lithography and developing. The wafer was further etched by SF₆ with Inductively Coupled Plasma Etch (ICP) to transfer the XMU pattern on to silicon nitride to expose subjacent silicon surface. Finally the wafer was soaked in acetone to remove the photoresist. The patterned chip was operated in the procedure described above to construct AuNP-Si system.

Raman experiment: All Raman spectra were recorded on a XploRA Raman System. The power at the sample location was 2.42 mW excited with 638 nm laser line and the integration time was 20 s. The laser light was focused onto the sample using 50×L objective lens (Leica microscope). *p*-nitrothiophenol (*p*-NTP) was adsorbed onto the AuNPs-Si surface by soaking in a 5 mM solution in ethanol for 30 min. The samples were then rinsed with ethanol, and left to dry in argon flow for 1 min before measurement.

Results and discussion

Characterization of functionalized Si(111)-H surface. After the formation of the Si(111)-H surface, the surface was functionalized by photografting of 3-MPA molecules at room temperature as detailed in Scheme 1 (step B→C). The modified surface was characterized using X-ray photoelectron spectroscopy (XPS) to obtain the binding energies of C, S, and Si elements. Figure 1 shows the C1s, S2p and Si2p regions of the resulting XPS spectra of the 3-MPA-modified Si(111) surface (step C). Examining the C1s XPS spectrum, a major peak at 285.2 eV can be attributed to the -CH₂-, which is consistent with recent studies.³¹⁻³³ The shoulder peak at 286.1 eV can be attributed to the alcohol carbon (C-O) of the 3-MPA-modified Si(111).^{34, 35} According to the XPS spectrum, we can estimate the atomic ratio of the two types of carbon to nearly 2:1, corresponding to the theoretical ratio. As shown in Fig. 1b, the S2p XPS spectrum shows typical S peaks at 168.3 eV and 170.2 eV, fitted by a doublet of Voigt peaks with fixed intensity ratio of S2p_{3/2}: S2p_{1/2} = 2:1. This shows that the S-H bond keeps well.^{36, 37} The doublet peaks found at 99.8 and 100.6 eV are in good agreement with the Si2p_{3/2} and Si2p_{1/2} in the expected 2:1 area ratio (Figure 1c). In particular, the silicon spectrum also displays a weak broad peak within the region of 102-105 eV. We assigned this peak to the formation of the Si-O bonds, which is consistent with a previous study.^{38, 39}

The XPS data clearly demonstrate that 3-MPA molecules were grafted on the Si(111)-H surface via the C=O carboxyl group by forming Si-O-C bonds. The S-H bond of 3-MPA molecule was well maintained after photografting on the Si(111)-H surface. To give an intuitive view, Figure 1(d) shows the analyzed grafted structure of 3-MPA on Si(111)-H surface.

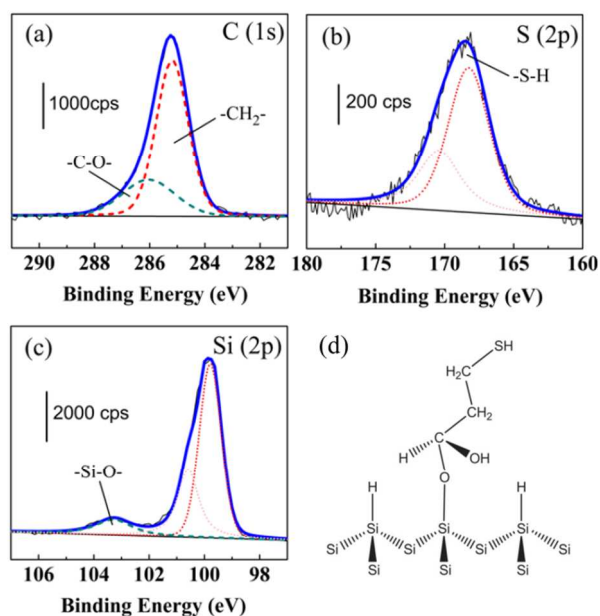


Figure 1. X-ray photoelectron region spectra of a monolayer of 3-MPA grafted on a Si(111)-H surface prepared by the method of white-light irradiation. (a) C 1s, (b) S 2p, (c) Si 2p and (d) the analyzed grafted structure of 3-MPA on Si(111)-H surface.

AuNPs in-situ growth. Figure 2 shows the SEM images of AuNPs grown on 3-MPA-modified silicon surfaces under different conditions (step C→D in Scheme 1) and the size distribution correspondingly. It can be concluded that the grafted 3-MPA molecules successfully catalyze Au⁺ ions in solution phase reduced into AuNPs on Si(111) surface. The coverage of AuNPs increased with the concentration of Au⁺ and the treatment time. As shown in Figure 2(a), the AuNPs were in the size of approximately 10 nm. Double the treatment time, the particle size enlarged into 11 nm. The AuNPs would be 15 nm, if the concentration of Au⁺ in solution phase was doubled. When we double the concentration of Au⁺ and the treatment time, the size of AuNPs would be enlarged into 21 nm. On this condition, as the 3-MPA-modified Si(111) wafers were placed into a solution of 5 mM KAu(CN)₂ and heated at 90°C for 20 min, the AuNPs grew in a closely packed manner on the modified surface and there were few vacant spaces between these AuNPs. According to the statistical analysis, the size distribution of AuNPs is uniform, approximately 10, 11, 15, and 21 nm in diameter under various conditions. As mentioned before, only small nanoparticles with dimensions below 20 nm can efficiently generate hot electrons with large energies.¹⁶ Thus, it is meaningful that the packing and size of these small AuNPs can be, to a large extent, influenced by the concentration of Au⁺ and the treatment time.

It should be emphasized that AuNPs cannot be obtained from Au(CN)₂⁻ ions on either the cleaned Si(111) surface or the hydrogen-terminated Si(111) surface without molecular modification (see Figure S1 in Supporting Information). This further proves that the dense grafting of 3-MPA molecules onto the Si(111)-H surface is the key step to successfully catalyze

$\text{Au}(\text{CN})_2^-$ ions reduced into AuNPs on Si(111) surface. The whole catalyzing AuNPs growth mechanism is inferred as follows: $\text{Au}(\text{CN})_2^-$ ions are first captured by the resultants of modified 3-MPA molecules on the silicon surface, and are superveniently reduced to atoms by the molecular functional groups ($-\text{S}-\text{H}$ or $\text{Si}-\text{O}-\text{C}(-\text{R})-\text{O}-\text{H}$). Several surface bonding atoms are aggregated into a crystal nucleus to catalyze the reduction process of Au^+ ions in the surrounding solution by the reducing agents (potassium citrate and citric acid). As the reaction proceeds in an elevated temperature, the initial nucleation sites can grow rapidly to form AuNPs on the Si surface in few minutes.

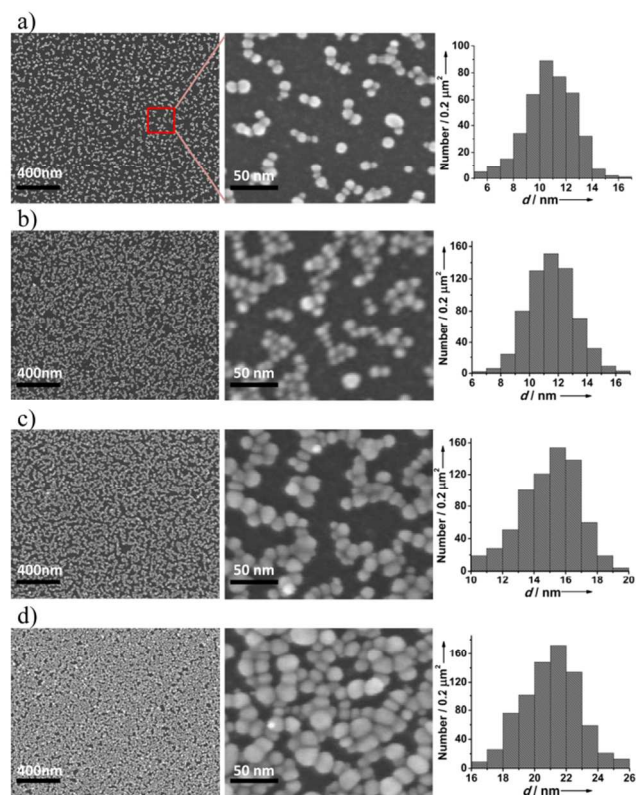


Figure 2. Scanning electron microscopy (SEM) images and the size distribution of AuNPs grown on 3-MPA-modified Si surfaces under different conditions. a) SEM images of the AuNPs with a size of approximately 10 nm, and the corresponding size distribution. b) SEM images of the AuNPs with a size of approximately 11 nm, and the corresponding size distribution. c) SEM images of the AuNPs with a size of approximately 15 nm, and the corresponding size distribution. d) SEM images of the AuNPs with a size of approximately 21 nm, and the corresponding size distribution. The electroless deposition solution contained $\text{KAu}(\text{CN})_2$, potassium citrate, and citric acid. The amount of potassium citrate and citric acid kept constant. a) 2.5 mM $\text{KAu}(\text{CN})_2$, 10 min; b) 2.5 mM $\text{KAu}(\text{CN})_2$, 20 min; c) 5 mM $\text{KAu}(\text{CN})_2$, 10 min; d) 5 mM $\text{KAu}(\text{CN})_2$, 20 min.

The AuNPs can grow selectively in a certain region on a patterned chip. A patterned chip was fabricated by the process flow provided in Supporting Information (Figure S2). Figure 3 shows the metallographic microscopy image of the patterned Si- Si_3N_4 chip and SEM images of the chip after the treatment according to Scheme 1. It can be seen that the method detailed in Scheme 1 produces selective growth of AuNPs on the patterned chip. Specifically, the AuNPs could not be grown on a silicon nitride (Si_3N_4) surface, but were grown well on the exposed Si(111)-H surface modified with 3-MPA. Moreover, we also found that these AuNPs did not detached from the prepared surface even when the sample was sonicated in mesitylene, indicating that the AuNPs were firmly bonded to the Si(111) surface. Therefore, it was clear from these results that in-situ growth of small size of AuNPs on the silicon-based devices can be certainly realized using the reported method.

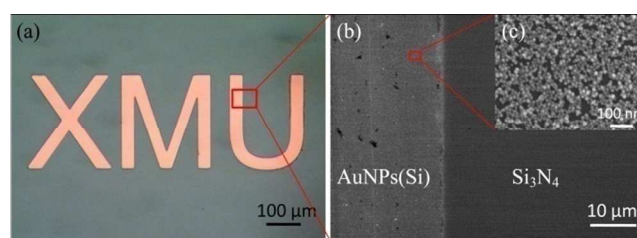


Figure 3. Metallographic microscopy image (a) and SEM images (b), (c) of a patterned Si- Si_3N_4 chip; AuNPs grew selectively on Si region using the method detailed in Scheme 1. (a) The pink areas (XMU) are the constructed AuNP-molecule-Si system and the dark green area is silicon nitride (Si_3N_4). The 3-MPA-modified Si(111) patterned chip was put into an electroless deposition solution contained of $\text{KAu}(\text{CN})_2$ (5 mM), potassium citrate (77 mM) and citric acid (32 mM) for 20 min to obtain AuNPs.

Surface-enhanced Raman scattering (SERS) enhancement of the AuNP-Si substrate. Since the AuNPs grew selectively on the patterned Si- Si_3N_4 chip in a closely packed manner, it is very interesting to evaluate its SERS enhancement.^{40, 41} And *p*-NTP was used as the probe.⁴² Figure 4 shows the SERS spectrum of 5×10^{-4} M *p*-NTP molecules adsorbed on the constructed AuNP-Si substrate and the spectrum of the substrate. The observed Raman bands that are assigned to *p*-NTP include ring stretching mode at 1572 cm^{-1} , symmetric stretching mode of the nitro group at 1336 cm^{-1} , C-H bending mode at 1110 cm^{-1} , C-S stretching mode at 1080 cm^{-1} .⁴³ A minor background signal from the substrate marked in red can also be observed in the SERS spectrum. The marked band around $916\text{--}1005 \text{ cm}^{-1}$ is attributed to the silicon bulk as observed in spectrum (b). The Raman peaks of *p*-NTP molecules are so prominent that the background signal can be negligible.

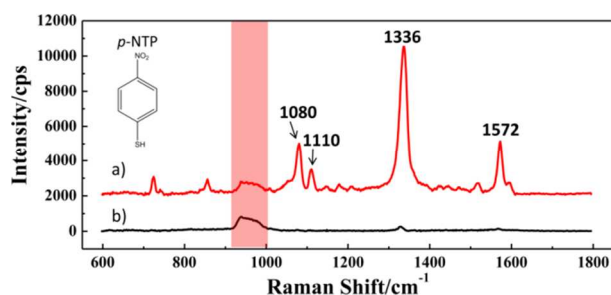


Figure 4. (a) SERS spectrum of *p*-nitrothiophenol (*p*-NTP) on the AuNP-Si substrate. (b) The Raman spectrum of the constructed AuNP-Si substrate. The 3-MPA-modified Si(111) chip was put into an electroless deposition solution contained of $\text{KAu}(\text{CN})_2$ (5 mM), potassium citrate (77 mM) and citric acid (32 mM) for 20 min to obtain AuNPs.

Theoretical simulation. Since the photografting of 3-MPA molecules onto the Si(111)-H surface is a key step for subsequence, it is meaningful to further understand the addition reaction of 3-MPA molecules with the Si(111)-H surface under white-light irradiation.

The reaction pathway for this process is proposed in Figure 5. Under white light irradiation, some special localized electron [e^-]/hole [h^+] pairs are activated on the Si(111)-H surface. The surface sites with the positive charge population may be attacked by the carbonyl π -electrons to form the Si-O bond. Meanwhile, the hydrogen atom attacks the carbon atom of carbonyl group to form the C-H bond. DFT calculations were conducted to verify the rationale of the proposed reaction mechanism. The cluster model $\text{Si}_{24}\text{H}_{36}$ was used to mimic the hydrogenated silicon surface, reproducing a portion of the Si(111)-H surface. In the cluster model, hydrogen atoms were used to terminate the dangling bonds due to the surface silicon atoms (twelve nearest neighbor on-top reaction sites). This condition also satisfied the tetrahedral sp^3 bonding environment of the silicon atoms. DFT calculations with B3LYP functional,⁴⁴⁻⁴⁶ combined with the 6-311+G** full-electron basis set were performed using the Gaussian 09 package.⁴⁷

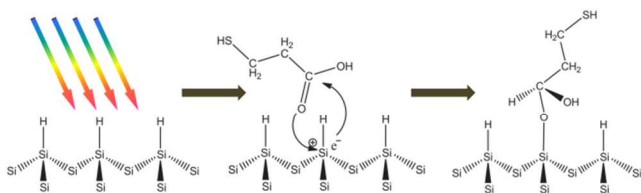


Figure 5. Proposed mechanism of white-light initiated 3-MPA grafting on hydrogen-terminated Si(111) surface.

Figure 6 presents the reaction potential energy surfaces for the singlet ground state (S_0 , bottom) and the first singlet excited state (S_1 , top). The ground state reaction path was first determined by finding the minima and the saddle points corresponding to reactants, transition state (TS) and product on

the potential energy curve (PEC). Full optimization without any geometry constraints was performed in DFT calculations. Vibrational frequency analysis was performed to confirm the right intermediates and transition state along the reaction coordination. The first vibrational frequency values of reactants, transition state and product are predicted to be 2.6, 806.5i and 9.2 cm^{-1} , respectively. Geometrical parameters of relevant states have been provided in Supporting Information (Table S1-4). And Table S5 gives the calculated natural bonding orbital (NBO) charge for transition state (TS) on the potential energy curve in the S_0 state, revealing the negatively charged hydrogen atom and the positively charged silicon atom in the four-member ring. For the S_0 state, the heat of reaction and the activation barrier energy are -0.36 eV and 2.10 eV, respectively. This indicates that the grafted reaction is kinetically disadvantageous due to the large activation energy barrier. The data show that in S_0 the reaction presents a very small heat of reaction and a huge activation barrier, confirming the implausibility of thermal activation for this process. Consequently, the grafting of 3-MPA as a photochemical reaction became the focus of our attention.

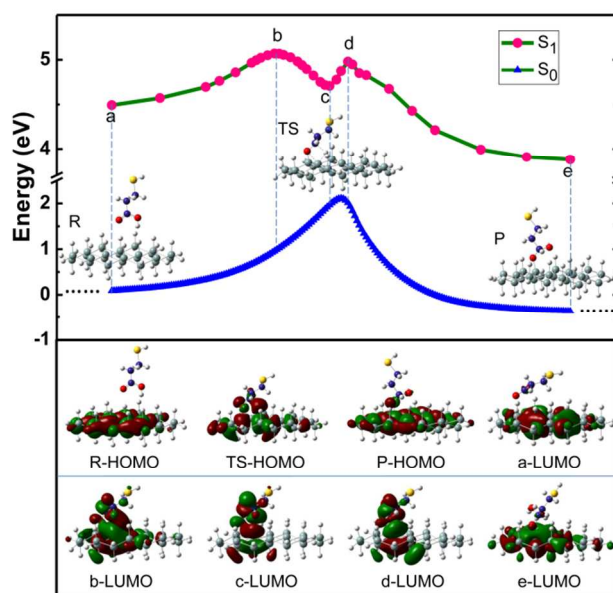


Figure 6. Calculated reaction paths for the addition of 3-MPA to $\text{Si}_{24}\text{H}_{36}$ cluster. The energies were calculated at the ground state S_0 and the first excited state S_1 . The inserted images correspond to the optimized structures of reactants, transition state, and product on the potential energy curve in the ground state S_0 . The images in the bottom show the highest occupied molecular orbital (HOMO) of R, TS and P on the S_0 PEC, and the lowest unoccupied molecular orbital (LUMO) of some marked point along the reaction coordinate.

To explore the influence of light, the potential energy curve of the first singlet excited state (S_1) was calculated using the time-dependent DFT approach (TD-B3LYP) along the reaction coordinate at the S_0 state. Geometry optimization and frequency

calculations were not performed to examine the nature of the S_1 state potential surface in the vicinity of a, b, c, d and e geometries in S_0 state. As the probe molecule and the cluster model are so large, we employ the TD-DFT calculation to estimate the reaction possibility qualitatively based on the geometries along the reaction path in the ground states on the basis of a vertical approximation. Since the gap between the valence and conduction bands of the Si(111)-H surface is experimentally measured to be about 1.1~1.3 eV,³² visible light can excite the hydrogen-terminated silicon. To reduce the computational cost, the silicon surface was modeled as a single-layer $Si_{24}H_{36}$ cluster. As the optical gap has high dependence on the size of cluster,⁴⁸⁻⁵⁰ the transition energy is larger than the experimental values, similar to many previous theoretical studies.^{32, 51}

Table 1. Energies (in eV) of relevant states at the ground state S_0 and the first excited state S_1 in the addition reaction of 3-MPA molecules with the Si(111)-H surface

	S_0		S_1
R	0	a	4.49
TS	2.10	b	5.07
P	-0.36	c	4.71
--	--	d	4.98
--	--	e	3.87

By considering the absorption of white light, the reaction can be activated with a sharp decline of the energy barrier in singlet excited states. Our TD-B3LYP results show that at the S_1 PEC,⁵¹⁻⁵³ a new intermediate can be formed, where the two reaction barriers decrease significantly to 0.58 eV and 0.27 eV compared with 2.10 eV of the S_0 . Figure 6 also shows the electron cloud distribution changes accordingly along the reaction coordinator at the potential energy surface of the S_0 state. For the reactants (R), the HOMO mainly displays a population on the Si atoms; while for the product (P), it partially populates in the grafted 3-MPA. The (TS) state is a four-member-ring configuration that is unstable due to the large ring tension. The electron cloud of the (TS) also shows that there is a weak bonding interaction between adsorbate and the $Si_{24}H_{36}$ cluster. Thus the activation energy barrier in the S_0 PEC is relatively high. By contrast, when the reactants absorbed photonic energy, they were excited to the S_1 state with a large oscillator strength ($f = 0.033$). Then the excited reactants can readily surmount a lower energy barrier with 0.58 eV to form a new four-member-ring intermediate which is relatively stable due to the π^* bonding effect localized in the ring (see electron cloud distribution c-LUMO in Figure 6). The intermediate can easily surmount the lower energy barrier of 0.27 eV to be

transformed to the excited product, in which there exists a strong σ bonding with the Si–O bond. Furthermore, the Gibbs free energy of the product is around 0.62 eV lower than that of reactants in the S_1 state. The product then relaxes back to the S_0 state of the final product.

Our calculations showed that the additional reaction mechanism follows some special localized electron [e^-]/hole [h^+] pairs activated on the Si(111)-H surface induced by white light. The surface sites with the positive charge population are attacked by the carbonyl π -electrons to form the Si–O bond. Meanwhile, the negatively charged hydrogen atom attacks the carbon atom of carbonyl group to form the C–H bond. Our results of DFT calculations are undoubtedly very helpful to understand the photochemical mechanism for photografting of organic molecules on semiconductor surfaces.

Conclusions

In summary, we designed a novel, mild and effective method for grafting of high-quality organic monolayers on silicon surface to catalyze small nanoparticles growth. By using white light source, 3-MPA molecules were attached to Si(111)-H surface at room temperature. XPS results confirmed the formation of the grafted Si–O bonds on the 3-MPA-modified Si(111) surfaces. The AuNPs grown on this functionalized surface have high uniformity and compactness. Our experiments also demonstrated that AuNPs can grow selectively in a certain region on a patterned Si-Si₃N₄ chip. The high-density gold nanoparticles substrate with a well reproducibility of the surface-enhanced Raman signal, can serve as molecular detections.

The 3-MPA molecules grafted onto the Si(111)-H surface is the key step in the successful catalysis AuNPs in-situ growth. To better understand the mechanism of the photografting of 3-MPA on the Si(111)-H surface, DFT calculations were performed and the theoretical results indicated that the formation of the Si–O bond occurred at the PEC of the S_1 state with a very low activation barrier about 30% of the ground state (S_0) value. The reported strategy can be applied to the design of high-performance electronic/photonic devices by combining the synthetic advantages of small size of AuNPs and silicon as well as the controllable functional versatility of molecules.

Acknowledgements

This work was supported by the National Science Foundation of China (NSFC) (No. 21373172), Innovation Group of Interfacial Electrochemistry (No. 21321062), and MOST (No. 2011YQ03012400).

Notes and references

State Key Laboratory of Physical Chemistry of Solid Surfaces and Department of Chemistry, College of Chemistry and Chemical Engineering, Xiamen University, Xiamen, 361005, China. E-mail: dywu@xmu.edu.cn; fzyang@xmu.edu.cn; Tel: +86-592-2189023.

Electronic Supplementary Information (ESI) available: SEM images of the cleaned Si(111) surface or the Si(111)-H surface without molecule

- modifying after immersed in electroless deposition solution; schematic plots for fabricating a patterned chip; and calculated parameters with the DFT method at the B3LYP/6-311+G** level. See DOI: 10.1039/b000000x/
- 1 D. H. Wan, H. L. Chen, T. C. Tseng, C. Y. Fang, Y. S. Lai, F. Y. Yeh, *Advanced Functional Materials* **2010**, *20*, 3064-3075.
 - 2 M. Losurdo, M. M. Giangregorio, G. V. Bianco, A. Sacchetti, P. Capezuto, G. Bruno, *Solar Energy Materials and Solar Cells* **2009**, *93*, 1749-1754.
 - 3 D. Hojo, T. Togashi, D. Iwasa, T. Arita, K. Minami, S. Takami, T. Adschiri, *Chemistry of Materials* **2010**, *22*, 1862-1869.
 - 4 O. Yaffe, L. Scheres, S. R. Puniredd, N. Stein, A. Biller, R. H. Lavan, H. Shpaisman, H. Zuilhof, H. Haick, D. Cahen, A. Vilan, *Nano Letters* **2009**, *9*, 2390-2394.
 - 5 M. W. Knight, H. Sobhani, P. Nordlander, N. J. Halas, *Science* **2011**, *332*, 702-704.
 - 6 M. Grätzel, *Nature* **2001**, *414*, 338-344.
 - 7 S. M. Sze, K. K. Ng, *Physics of semiconductor devices*. Editor, John Wiley & Sons, **2006**.
 - 8 H. A. Atwater, A. Polman, *Nature Materials* **2010**, *9*, 205-213.
 - 9 R. Elghanian, J. J. Storhoff, R. C. Mucic, R. L. Letsinger, C. A. Mirkin, *Science* **1997**, *277*, 1078-1081.
 - 10 C. L. Nehl, H. W. Liao, J. H. Hafner, *Nano Letters* **2006**, *6*, 683-688.
 - 11 G. Raschke, S. Kowarik, T. Franzl, C. Sonnichsen, T. A. Klar, J. Feldmann, A. Nichtl, K. Kurzinger, *Nano Letters* **2003**, *3*, 935-938.
 - 12 Y. W. C. Cao, R. C. Jin, C. A. Mirkin, *Science* **2002**, *297*, 1536-1540.
 - 13 J. A. Schuller, E. S. Barnard, W. Cai, Y. C. Jun, J. S. White, M. L. Brongersma, *Nature Materials* **2010**, *9*, 193-204.
 - 14 S. Mukherjee, F. Libisch, N. Large, O. Neumann, L. V. Brown, J. Cheng, J. B. Lassiter, E. A. Carter, P. Nordlander, N. J. Halas, *Nano Letters* **2012**, *13*, 240-247.
 - 15 I. Thomann, B. A. Pinaud, Z. Chen, B. M. Clemens, T. F. Jaramillo, M. L. Brongersma, *Nano Letters* **2011**, *11*, 3440-3446.
 - 16 A. O. Govorov, H. Zhang, Y. K. Gun'ko, *The Journal of Physical Chemistry C* **2013**, *117*, 16616-16631.
 - 17 M. T. Sheldon, J. van de Groep, A. M. Brown, A. Polman, H. A. Atwater, *Science* **2014**, *346*, 828-831.
 - 18 J. M. Buriak, *Chemical Reviews* **2002**, *102*, 1271-1308.
 - 19 S. Ciampi, J. B. Harper, J. J. Gooding, *Chemical Society Reviews* **2010**, *39*, 2158-2183.
 - 20 H. Sugimura, S. H. Mo, K. Yamashiro, T. Ichii, K. Murase, *Journal of Physical Chemistry C* **2013**, *117*, 2480-2485.
 - 21 Y. J. Song, Y. Wang, B. B. Li, C. Fernandes, H. E. Ruda, *Nanoscale* **2013**, *5*, 6779-6789.
 - 22 Y. J. Song, Z. S. Zhang, H. E. Elsayed-Ali, H. N. Wang, L. L. Henry, Q. Q. Wang, S. L. Zou, T. Zhang, *Nanoscale* **2011**, *3*, 31-44.
 - 23 Y. J. Song, W. T. Yin, Y. H. Wang, J. P. Zhang, Y. Wang, R. M. Wang, J. B. Han, W. Wang, S. V. Nair, H. E. Ruda, *Scientific reports* **2014**, *4*, 4991..
 - 24 P. E. Colavita, B. Sun, K. Y. Tse, R. J. Hamers, *Journal of the American Chemical Society* **2007**, *129*, 13554-13565.
 - 25 B. J. Eves, Q. Y. Sun, G. P. Lopinski, H. Zuilhof, *Journal of the American Chemical Society* **2004**, *126*, 14318-14319.
 - 26 R. Boukherroub, D. D. M. Wayner, *Journal of the American Chemical Society* **1999**, *121*, 11513-11515.
 - 27 T. Hentschel, D. Isheim, R. Kirchheim, F. Muller, H. Kreye, *Acta Materialia* **2000**, *48*, 933-941.
 - 28 Y. He, Y. L. Zhong, F. Peng, X. P. Wei, Y. Y. Su, S. Su, W. Gu, L. S. Liao, S. T. Lee, *Angewandte Chemie-International Edition* **2011**, *50*, 3080-3083.
 - 29 X. M. Shen, Y. J. Song, S. Li, R. S. Li, S. X. Ji, Q. Li, H. P. Duan, R. W. Xu, W. T. Yang, K. Zhao, R. Rong, X. Y. Wang, *Rsc Advances* **2014**, *4*, 34179-34188.
 - 30 L. A. Huck, J. M. Buriak, *Journal of the American Chemical Society* **2012**, *134*, 489-497.
 - 31 P. Bertani, X. J. Wen, W. Lu, *Journal of Electronic Materials* **2012**, *41*, 830-836.
 - 32 X. Y. Wang, R. E. Ruther, J. A. Streifer, R. J. Hamers, *Journal of the American Chemical Society* **2010**, *132*, 4048-4049.
 - 33 Y. L. Zhong, S. L. Bernasek, *Journal of the American Chemical Society* **2011**, *133*, 8118-8121.
 - 34 C. K. Chan, R. Ruffo, S. S. Hong, Y. Cui, *Journal of Power Sources* **2009**, *189*, 1132-1140.
 - 35 Q. Y. Sun, L. de Smet, B. van Lagen, A. Wright, H. Zuilhof, E. J. R. Sudholter, *Angewandte Chemie-International Edition* **2004**, *43*, 1352-1355.
 - 36 Y. H. Lai, C. T. Yeh, C. C. Yeh, W. H. Hung, *Journal of Physical Chemistry B* **2003**, *107*, 9351-9356.
 - 37 T. Ishida, N. Choi, W. Mizutani, H. Tokumoto, I. Kojima, H. Azebara, H. Hokari, U. Akiba, M. Fujihira, *Langmuir* **1999**, *15*, 6799-6806.
 - 38 A. Bansal, X. L. Li, I. Lauermaun, N. S. Lewis, S. I. Yi, W. H. Weinberg, *Journal of the American Chemical Society* **1996**, *118*, 7225-7226.
 - 39 R. Miao, L. X. Mu, H. Y. Zhang, H. T. Xu, B. J. Zhou, G. W. She, P. F. Wang, W. S. Shi, *Acs Applied Materials & Interfaces* **2013**, *5*, 1741-1746.
 - 40 O. Bisi, S. Ossicini, L. Pavesi, *Surface Science Reports* **2000**, *38*, 1-126.
 - 41 J. H. Park, L. Gu, G. von Maltzahn, E. Ruoslahti, S. N. Bhatia, M. J. Sailor, *Nature Materials* **2009**, *8*, 331-336.
 - 42 H. Foll, M. Christophersen, J. Carstensen, G. Hasse, *Materials Science & Engineering R-Reports* **2002**, *39*, 93-141.
 - 43 B. Skadatchenko, R. Aroca, *Spectrochimica Acta Part A: Molecular and Biomolecular Spectroscopy* **2001**, *57*, 1009-1016.
 - 44 A. D. Becke, *Physical Review A* **1988**, *38*, 3098-3100.
 - 45 A. D. Becke, *Journal of Chemical Physics* **1993**, *98*, 5648-5652.
 - 46 C. T. Lee, W. T. Yang, R. G. Parr, *Physical Review B* **1988**, *37*, 785-789 10.1103/PhysRevB.37.785.
 - 47 M. J. Frisch, G. W. Trucks, H. B. Schlegel, G. E. Scuseria, M. A. Robb, J. R. Cheeseman, G. Scalmani, V. Barone, B. Mennucci, G. A. Petersson, et al. Gaussian 09, Revision A.02, Gaussian, Inc., Wallingford, CT, USA, **2009**.
 - 48 C. J. Barrelet, D. B. Robinson, J. Cheng, T. P. Hunt, C. F. Quate, C. E. D. Chidsey, *Langmuir* **2001**, *17*, 3460-3465.
 - 49 T. Vondrak, X. Y. Zhu, *Physical Review Letters* **1999**, *82*, 1967-1970.
 - 50 F. Effenberger, G. Gotz, B. Bidlingmaier, M. Wezstein, *Angewandte Chemie-International Edition* **1998**, *37*, 2462-2464.
 - 51 M. Cossi, A. Bocchia, A. G. Marrani, R. Zanon, *Journal of Physical Chemistry C* **2011**, *115*, 19210-19215.

52 Y. Kanai, A. Selloni, *Journal of the American Chemical Society* **2006**, *128*, 3892-3893.

53 A. Puzder, A. J. Williamson, J. C. Grossman, G. Galli, *Physical Review Letters* **2002**, *88*, 097401.

